Available online at www.sciencedirect.com

ScienceDirect

journal homepage: www.elsevier.com/locate/he

Cycling performance and hydriding kinetics of $LaNi_5$ and $LaNi_{4.73}Sn_{0.27}$ alloys in the presence of CO

E.M. Borzone [a,*], M.V. Blanco [a,b], G.O. Meyer [a,c], A. Baruj [a,c]

[a] Centro Atómico Bariloche/Instituto Balseiro, CNEA/U.N. Cuyo, Av. Bustillo 9500, 8400 Bariloche, Argentina
[b] Agencia Nacional de Promoción Científica y Tecnológica (ANPCyT), Argentina
[c] Consejo Nacional de Investigaciones Científicas y Técnicas (CONICET), Argentina

ARTICLE INFO

Article history:
Received 30 January 2014
Received in revised form
21 April 2014
Accepted 2 May 2014
Available online 28 May 2014

Keywords:
Metal hydride
AB5
Sn
Purification
Poisoning
Carbon monoxide

ABSTRACT

We analyzed the sorption cycling behavior of $LaNi_5$ and $LaNi_{4.73}Sn_{0.27}$ alloys in H_2 containing 10 and 100 ppm of CO. The effect of temperature was studied for the Sn-containing alloy. When cycling in the presence of CO, we found the reaction was strongly retarded due to surface contamination but no loss of capacity was observed when samples were given enough time for both absorption and desorption. The retardation was stronger at lower temperatures and higher CO concentration. The results also indicate that a fraction of the adsorbed CO is released during the desorption process. For the Sn-containing alloy, a stationary state is met after about 10 cycles, with no further degradation occurring past this point. The retarding factor at 40 °C and 100 ppm in this condition, with respect to the kinetics in pure hydrogen, is of about 600.

Introduction

The effect of the impurities potentially present in the hydrogen stream is one of the key engineering considerations when designing devices based on hydride forming materials (HFM). Besides interfering with the general process [1], contamination of the HFM usually affects the reaction and could even prevent it from taking place [2]. For this reason, many applications require the use of high purity hydrogen [3] or the incorporation of additional purification stages prior to the final use [4]. One particular case is the application of HFM to hydrogen purification processes, where the selective nature of the reaction is used to separate hydrogen from other gases or impurities. This kind of process necessarily exposes the HFM to possible contaminants, thus lending importance to the understanding on how these contaminants affect the hydrogen sorption behavior.

Among the commonly found impurities in industrial applications, carbon monoxide is known to have a particularly adverse effect on most metallic HFM, including AB_5 alloys. CO molecules interact with the alloys surface, hampering the subsequent reaction [5,6]. The resulting behavior, often called surface poisoning, has been described in terms of a sorption

* *Corresponding author*. Centro Atómico Bariloche, Av. Bustillo 9500, 8400 Bariloche, Argentina. Tel.: +54 294 4445278.
E-mail addresses: manque.borzone@gmail.com, emiliano.borzone@ib.edu.ar (E.M. Borzone).
http://dx.doi.org/10.1016/j.ijhydene.2014.05.004

capacity that exponentially decreases with the number of absorption–desorption cycles [2,7]. In the case of $LaNi_5$, this effect can be reversed by means of a thermal treatment under dynamical vacuum [8] or by cycling in pure H_2 [5,9].

The details of the poisoning process are not fully understood. According to a well established model, during activation and in the presence of traces of O_2, lanthanum oxides are formed and nickel precipitates into metallic clusters which configure the active sites for hydrogen dissociation [5]. The presence of metallic Ni clusters in samples subjected to several hydriding/dehydriding cycles has been confirmed by ferromagnetic resonance measurements [10]. The strong effect of CO could then be explained by its affinity for Ni surfaces [11] which interferes with the H_2 dissociation process. This mechanism is further supported by FTIR measurements of CO poisoned $LaNi_5$ suggesting that CO molecules adsorb on metallic Ni [6]. However, AES and XPS analyses show that no fresh Ni atoms exist on the $LaNi_5$ surface exposed to air or even low vacuum, as it is densely covered by a layer of oxides and hydroxides of the constituent elements that the hydrogen has to diffuse through [12]. Interestingly, for the case of $LaNi_{5-x}Sn_x$, the SnO_2 present on the surface of the alloy is easily reduced by hydrogen [13]. This reduction originates an oxygen-deficient oxide that could play a catalytic role in hydrogen dissociation, as suggested by the increased surface hydrogen reactivity of these alloys in the presence of O_2 and H_2O with respect to its clean surface [14]. This behavior is opposite to that observed for other AB_5 alloys [12] and suggests that $LaNi_{5-x}Sn_x$ alloys can be particularly interesting for hydrogen purification purposes.

Considering applications based on the use of HFM, impurities are usually detrimental for the system performance. In some cases, a possible strategy consists in removing harmful impurities from the gas stream before it gets in contact with the material. Such is the case of a hydrogen recovery plant built in China [15] where NH_3 and H_2O are separated from the feed gas before taking contact with the metal hydride beds. The same approach was implemented in a hydrogen purification system recently developed in Japan [16], in which CO impurities are eliminated upstream by an adsorption bed and then the hydrogen is separated from the other gases using HFM.

A different approach consists in performing various surface treatments on the HFM in order to improve their tolerance towards different impurities. Reported treatments include sol-gel encapsulating [17], ceramic encapsulating [18], Pd treatments [19–21], fluorination treatments [22–24] and hybrid variations [25,26]. This latter approach was used in a recently developed hydrogen separation prototype [27] where the feed gas contained up to 100 ppm of CO along with other less harmful impurities. In that case, the surface modification was carried out through fluorination followed by aminosilane functionalization and electroless deposition of Pd. All of these methods, to different degrees, increase the cost of the resulting alloy and compromise some hydrogen capacity in exchange for improved contamination resistance.

Finally, for specific target applications, the HFM could be used without additional treatments even in the presence of contaminating gases [28,29]. In such cases, it is necessary to determine how the reaction behavior would be affected by the contaminants in order to determine whether the overall performance is acceptable. Moreover, the HFM must be carefully studied under working conditions to adjust design parameters to the modified reaction behavior.

We are currently considering the use of $LaNi_{5-x}Sn_x$ alloys for the implementation of a metal hydride based low-pressure hydrogen separation device. In previous works we characterized the thermodynamics [30], hydrogen absorption kinetics [31] and pressure cycling stability [32] of such system for $0 \leq x \leq 0.5$. In one of the target applications the feed gas contains small amounts of CO (5–10 ppm). This concentration may be increased during the process due to the operation principle of the purification device. For this reason, it is necessary to characterize the effect of CO impurities on both the reaction rate and the hydrogen storage capacity of these materials under cyclic conditions.

One possible approach to this kind of study has been presented by Schweppe et al. [33]. These authors studied the effect of CO on the absorption kinetics of $LaNi_5$ by precovering the samples with known amounts of CO and other contaminants. After this precovering treatment, kinetic measurements were performed using pure hydrogen. This approach allows quantifying detrimental effects of the hydrogen sorption kinetics under constant surface coverage conditions. However, this situation is different to that found under working conditions, where the contaminant gets in contact with the sample surface together with the hydrogen gas. In real life conditions, CO coverage will change as cycling proceeds, affecting hydrogen sorption kinetics. For this reason, we prefer to approach this study by cycling initially clean samples using different gas mixtures. We analyze the cycling behavior of $LaNi_5$ and $LaNi_{4.73}Sn_{0.27}$ alloys in the presence of 10 and 100 ppm of CO at 40 °C. For the Sn-containing alloy the cycling is repeated at 90 °C.

Experimental details

Samples were prepared in buttons of about 10 g each by arc-melting pure La (99.9%), Ni (99.95%) and Sn (99%). The buttons were then encapsulated in quartz under Ar atmosphere

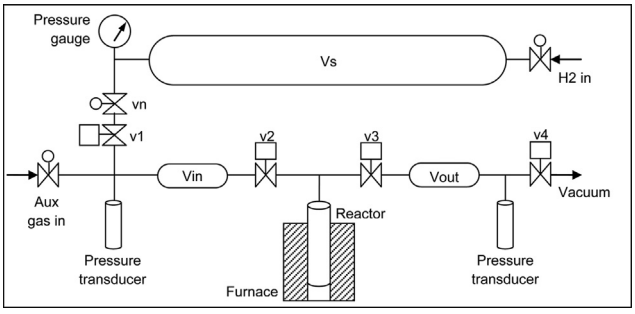

Fig. 1 – Diagram of the equipment used for cycling measurements. *Vs*, *Vin*, *Vout* are vessels. *vn*: Manual needle valve. *v1*, *v2*, *v3*, *v4*: Automatized solenoid valves. Samples are placed inside the reactor. Experiment control, and pressure/temperature data acquisition are performed with a PC.

and heat treated at 1223 K for 48 h. The resulting alloys were confirmed to be single-phase by X-ray diffraction, presenting a P6/mmm symmetry. Chemical analysis was performed on samples of each button by means of atomic absorption spectrophotometry to confirm the composition values. For details on the sample preparation procedure and the resulting characteristics of the alloys, see Ref. [30].

The device used for hydrogen absorption measurements is an open-ended cycling equipment developed at our laboratory, schematically shown in Fig. 1. The gas mixture (H_2 + CO) is contained in a 3800 cm^3 reservoir *Vs* connected to a calibrated absorption volume *Vin* of about 80 cm^3 through a needle valve *vn* in series with a solenoid valve *v1*. The starting pressure for each absorption is preset at 1000 kPa. This condition is achieved by opening *v1* and letting the pressure in *Vin* to rise in a controlled way. Typically, the preset value is reached within a margin of error of 4 kPa. Samples of about 1 g, previously activated in pure hydrogen and fully desorbed, were placed in a 304 L steel reactor. The calibrated reactor volume is around 10 cm^3. Temperature effects are accounted for during data processing. Each absorption begins when the reactor is put in contact with *Vin* by opening the solenoid valve *v2*. Hydrogen absorption is calculated from the pressure drop in the system according to Sieverts method. The absorption stage proceeds until a preset time is reached. For the desorption stage, *v2* is closed and solenoid valve *v3* is opened. As the material desorbs hydrogen, the pressure in volume *Vout* increases. During the desorption stage, this pressure is kept below 2 kPa by evacuating through solenoid valve *v4* in a controlled manner when necessary. In each case the absorption and desorption times were set at the same value. The process is repeated to cycle the sample. As the gas in *Vin* is not evacuated after each absorption, an increase in the CO concentration is expected during cycling. A simulation of the process has shown that the maximum concentration increase for 30 cycles in the conditions used would be of about 5%. Throughout the text, when CO compositions are stated they correspond to the initial value, i.e. the composition of the gas contained in *Vs*.

The gases used were grade 4.5 purity H_2 and H_2 containing either (101 ± 3) ppm or (10 ± 1) ppm of CO. The system pressure was measured using calibrated Baumer E914 transducers with a pressure range of 0–1600 kPa. The reactor temperature was regulated by means of a PID system with a 0.1 °C step connected to a 200 W Watlow furnace. The sample temperature was measured by means of a Pt-100 sensor placed in contact to the outer wall of the reactor. Differences between the reactor inner and outer temperatures were corrected by applying an experimentally determined calibration curve. Each cycling measurement was started at least 20 min after the reactor temperature stabilized. Experiment control and data acquisition were performed using a dedicated PC and a computer program developed in MS Visual Basic.

Results and discussion

Main results

Cycling hydrogen absorption results for $LaNi_{4.73}Sn_{0.27}$ at 40 °C are shown in Fig. 2. At 100 ppm CO (Fig. 2a) the first curve initially presents fast absorption kinetics up to about 0.7 wt.% (marked by an arrow in Fig. 2a), where the rate changes and the reaction transitions to a slower pace. Subsequent curves show a similar behavior, changing to a slower rate at progressively smaller reacted fractions. After about 10 cycles, a stationary state is reached where the complete absorption reaction takes place at a slow rate. No significant changes in the reaction kinetics are observed in further cycles. The observed outcome is that the absorption kinetics is about 600 times slower than that measured for the same alloy with pure H_2 under similar conditions [30,31]. The large experimental dispersion obtained in these curves could be related to the long time needed for measuring each one, of about 10 h. Even considering that ambient temperature was continually monitored and accounted for in calculations, its variations along the measuring period introduce a source of error in the experiments.

Notably, after 30 cycles the alloy hydrogen absorption capacity remains almost unchanged. No significant decrease in final hydrogen content is detected, in contrast to what is reported in the literature [2,7,22,34,35]. This difference could be related to the time allowed for the sample to absorb, as it will be discussed later on.

When cycling with H_2 containing 10 ppm CO (Fig. 2b), the shape of the curves is different but a stationary state is also met after 10 cycles. In this case, all the curves present a fast initial stage. When the stationary state is reached, the change in slope is found at a hydrogen content of about 0.8 wt.%.

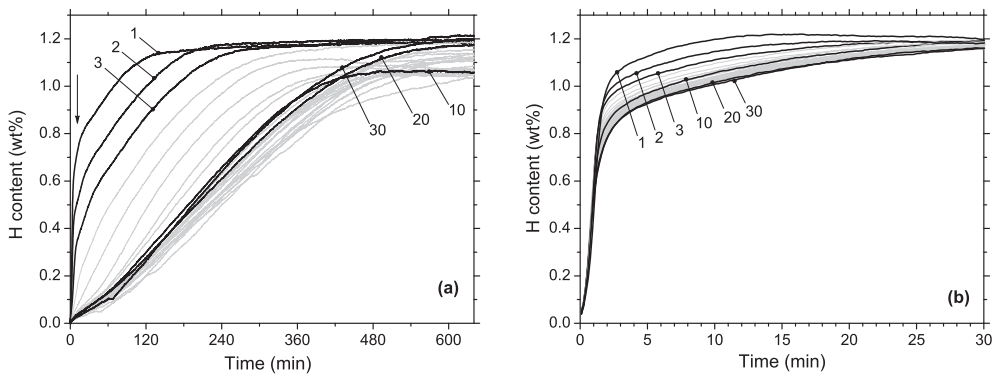

Fig. 2 – Cycling absorption kinetics of $LaNi_{4.73}Sn_{0.27}$ at 40 °C under (a): H_2 with 100 ppm CO and (b) H_2 with 10 ppm CO. Cycle numbers are indicated for selected curves.

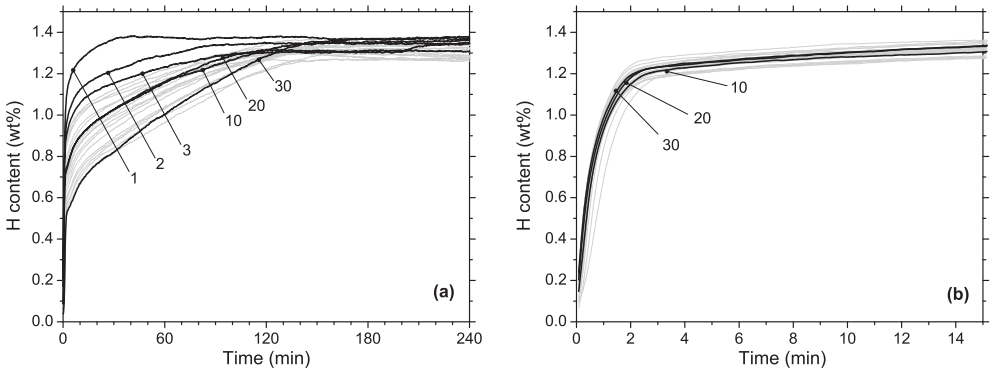

Fig. 3 – Cycling absorption kinetics of $LaNi_5$ at 40 °C under (a): H_2 with 100 ppm CO and (b) H_2 with 10 ppm CO. Cycle numbers are indicated for selected curves.

Again, cycling does not affect the alloy reversible capacity. To the best of our knowledge, this type of behavior has not been reported before.

A similar behavior is observed for $LaNi_5$, as shown in Fig. 3. In this case the reaction is faster than for the Sn-containing alloy although we note that for cycling under 100 ppm CO (Fig. 3a) a stationary state has not been established after 30 cycles and further degradation is likely to occur. For the measurements with 10 ppm CO a stationary state is observed after a few cycles. In this condition, kinetics presents a rather fast stage up to about 1.2 wt.% followed by a final slower rate of absorption up to the alloy complete capacity.

Fig. 4 summarizes the results found for total absorption capacity in terms of the number of cycles performed. Results obtained by cycling under pure H_2 are shown for comparison purposes [32]. In the case of $LaNi_{4.73}Sn_{0.27}$, the average final absorption capacity decreases with the increment of CO concentration. For each CO concentration, despite the rather large data dispersion, the total capacity does not show a decreasing tendency as cycling proceeds. In the case of $LaNi_5$, the absorption capacity remains essentially unchanged with CO concentration and during cycling. This result implies that, for applications where small amounts of CO are present, the alloys might be used with no further modification if slower reaction kinetics were acceptable and if this effect is taken into account in the design process.

The discussed behavior was observed after setting both absorption and desorption times long enough for the reaction to reach equilibrium. If the first condition is not met, then the final hydrogen content observed cannot be taken as a measure of the alloy capacity. It rather is a kinetic parameter indicating the reacted fraction at a given time. If the second condition is not met, then the alloy will not have been fully desorbed at the beginning of the next absorption stage. Although the reaction may reach equilibrium, the measured amount of hydrogen absorbed will be lower than the alloy capacity. This could be the case of the results presented in Refs. [2,7], which report a nearly exponential decrease in the capacity of the alloys with the cycle number, in Refs. [22,34], which report a strong decrease in capacity with no specific dependence, and in Ref. [35], which presents a poisoning model that yields a nearly linear dependence in capacity versus cycle. In the case of Ref. [34], the authors acknowledge that for one of the alloys the desorption reaction was not complete. Nevertheless, they interpreted cycling results in terms of a gradual decrease in the alloy hydrogen absorption capacity. Considering the experimental details of the mentioned references, the reason for the discrepancy between previous and current results could be due to an incomplete reaction in the former either in the absorption or the desorption stages. In order to clarify this point, measurements were performed for $LaNi_{4.73}Sn_{0.27}$ under H_2 containing 100 ppm CO at different temperatures and using

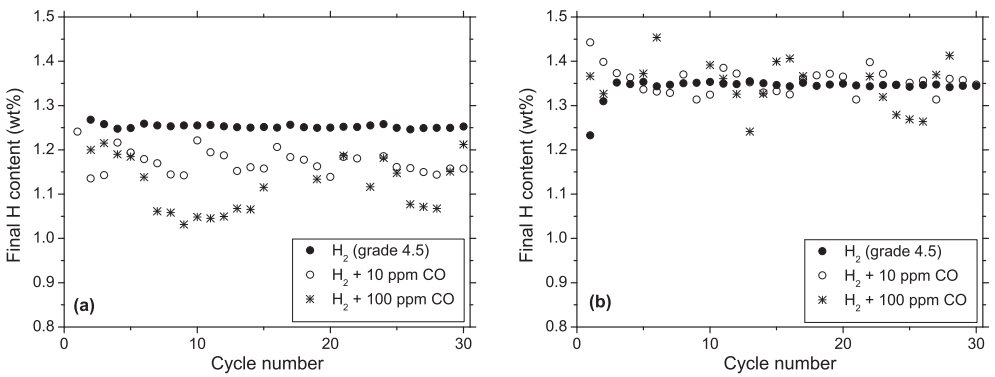

Fig. 4 – Final hydrogen content versus cycle number at 40 °C for: (a) $LaNi_{4.73}Sn_{0.27}$ and (b) $LaNi_5$. Different gas compositions are indicated.

fixed absorption and desorption times of 20 min Fig. 5 shows the H content recorded after 5 min for each case. In all cases, the initial trend is not far from a decreasing exponential dependence, in particular at lower temperatures. For higher temperatures, this tendency changes after only a few cycles. A similar behavior can be found in Ref. [5] for a $Fe_{0.85}Mn_{0.15}Ti$ alloy cycled at 25 °C under H_2 containing 300 ppm CO.

Temperature effect

Experiments were performed at 90 °C in order to examine the effect of temperature on the hydrogen absorption kinetics of $LaNi_{4.73}Sn_{0.27}$. The results for H_2 containing 100 and 10 ppm CO are presented in Fig. 6a and b, respectively. In the case of the gas containing a higher concentration of CO, the general behavior is similar to that discussed in previous paragraphs for ambient temperature experiments where a stationary state is reached after about 10 cycles. The main difference is that the kinetics observed at 90 °C is much faster than that obtained at lower temperatures for the same material.

For measurements with lower CO content a retard-recovery behavior is observed (Fig. 6b) [2]. This behavior is characterized by an initial kinetics degradation during the first 5 cycles, followed by an increment of the absorption rate at subsequent cycles. After about 20 cycles, a new stationary state is reached with a small loss of storage capacity. The retardation-recovery could be related with CH_4 formation that has been reported to take place on the surface of AB_5 alloys at temperatures over 100 °C [2,7]. The formation of CH_4 would help removing CO from the material surface [2,5,7,9]. If this were the case, CH_4 formation would also play a role in the higher concentration reactions shown in Fig. 6a, but it would be difficult to separate this role from the mentioned temperature effect on CO coverage. A proper explanation of this effect requires further research. It should be mentioned that, for hydrogen purification applications, higher temperatures lead to faster reaction kinetics although the possible CO desorption and CH_4 formation would be detrimental for the final product purity.

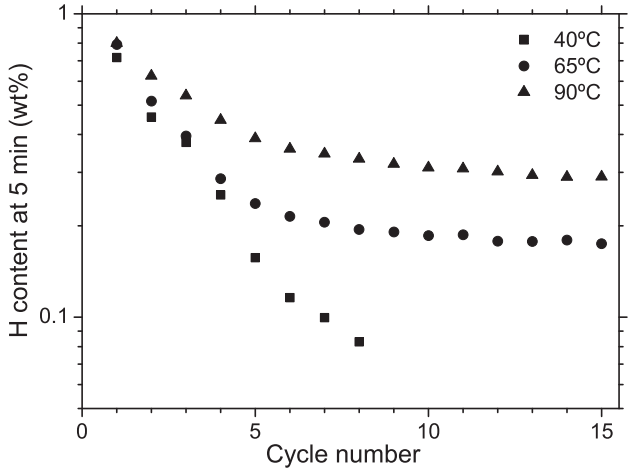

Fig. 5 – Hydrogen content at 5 min versus cycle number for $LaNi_{4.73}Sn_{0.27}$ for non-complete sorption cycles with H_2 and 100 ppm CO at different temperatures. Evolution at the early stages looks nearly exponential if the reaction is not given sufficient time to finish.

Microscopic interpretation

A common feature found in all measurements was an initial stage where the absorption rate is relatively fast, followed by a stage of lower kinetics. The change between these stages is somehow well defined and seen as a soft kink in the reaction curves (see for example the one marked by an arrow in Fig. 2a). Another common feature is that this kink occurs at lower reacted fractions as cycling proceeds until a stationary state is reached. A possible rationalization of this behavior is as follows. Under clean H_2 cycling conditions, the reaction kinetics for these materials are limited by bulk reactions [19,31,36,37]. Surface processes, in particular H_2 dissociation and chemisorption, occur at a faster rate at near equilibrium conditions. These surface processes take place at dissociation active sites, probably those were Ni atoms are present [6,11]. Experimental evidence shows that CO has a strong affinity for these sites too, and thus interferes with the hydrogen dissociation process [5,9]. Under the current experimental conditions, H_2 and CO molecules arrive at an initially clean surface and compete for the active sites. H_2 will dissociate and penetrate through the surface, while CO molecules will remain adsorbed onto the active sites. The surface will progressively become covered by CO molecules until there is a critical fraction of surface coverage where H_2 dissociation becomes the limiting step of the reaction kinetics. This change in the limiting mechanism could be the origin of the mentioned kink in the absorption curves. As reported by Schweppe et al. [38], a transition regime is expected between the bulk- and surface-limited stages. For this reason, the initial absorption rate is slower than for the case of pure H_2 and the transition point is not well defined, appearing as a soft kink in the curve. Upon completion of the absorption stage, active sites will be occupied by CO. If this coverage remained unchanged, one would expect a slow kinetics on the following absorption and further cycles. However, the fact that on the following cycle the initial rate is fast again indicates that at least part of the CO molecules are desorbed during the dehydriding process. This effect has already been described as surface recovery after poisoning of AB_5 alloys in the literature [5,8,9]. Those cases where the kink appears at progressively lower reacted fraction indicate that the surface recovery is not complete, and some CO remains adsorbed. As cycling proceeds, a dynamic equilibrium condition is met where the amount of CO adsorbed during H_2 absorption is similar to that desorbed during the H_2 desorption stage. This situation explains the final stationary state reached after some cycles. If at the stationary state the CO coverage after desorption is below the critical value, the faster initial stage will be observed during absorption, as it is the case of samples cycled with 10 ppm CO (Figs. 2b and 3b). On the other hand, if the steady-state coverage after desorption exceeds the critical value, the complete absorption reaction occurs at a slower rate, as shown in Fig. 2a ($LaNi_{4.73}Sn_{0.27}$, 100 ppm CO). In the case of $LaNi_5$ cycled with 100 ppm CO (Fig. 3a), the stationary state has not been reached after 30 cycles. A feature that could explain the different behavior between this material and the Sn containing alloy is the larger

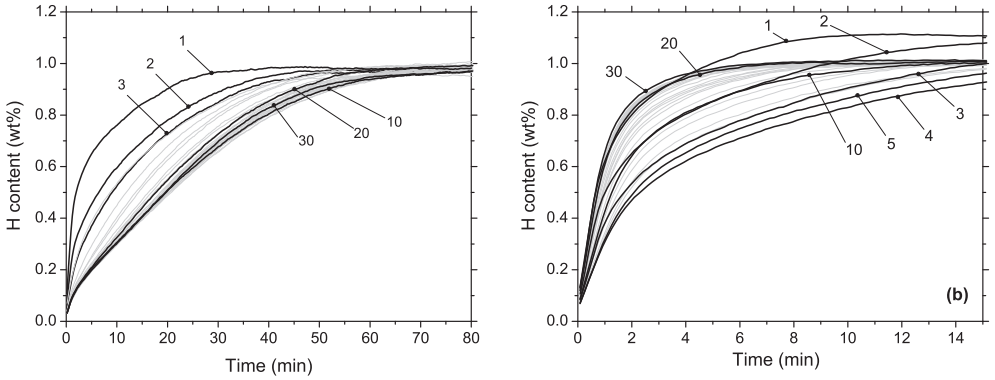

Fig. 6 – Absorption kinetics of $LaNi_{4.73}Sn_{0.27}$ for each cycle at 90 °C under (a): 100 ppm CO and (b) 10 ppm CO. Cycle number is indicated for selected curves.

lattice parameters of $LaNi_{5-x}Sn_x$ alloys. According to S. Han et al. [9], CO is adsorbed either at Ni-on-top or Ni–Ni-bridge sites with similar bonding energies. Increasing the lattice parameter could lead to a stronger bond between the CO molecule and the Ni–Ni-bridge site. This remains true for both $LaNi_5$ surface and metallic Ni clusters, which would contain some Sn in solid solution. Thus, more CO molecules will remain on the surface after desorption for the Sn-containing material in comparison to $LaNi_5$. The effect is reflected in the faster kinetics degradation and approach to the steady-state observed for the sample containing Sn (Figs. 2a and 3a). The kinetics model proposed by J.I. Han and J.Y. Lee [35] for H_2–CO gas has some features in common with the present interpretation of results. These authors proposed two possible models for the surface coverage: one where particles become completely inactive upon being contaminated by CO and another where each particle surface is partially affected by the presence of the contaminant. Present results resemble the simulations obtained with the second model [35], which lends support for the proposed explanation. However, Han and Lee considered surface reactions as the governing mechanisms for the sorption kinetics and thus, the model does not account for transitions in the absorption rate. In addition, as it was discussed in Main Results Section, supporting experiments were not performed until the completion of the absorption stage, which results in a seemingly progressive loss of capacity [35].

Reaction kinetics obtained at 90 °C are distinctly faster than those obtained at 40 °C. This is to be expected according to the previous interpretation, as CO desorption will be favored and therefore the stationary state at 90 °C is established at a lower CO coverage level than at 40 °C. Summarizing, the stationary CO coverage level decreases with temperature and increases with CO partial pressure.

Conclusions

We have studied the hydrogen absorption kinetics of $LaNi_5$ and $LaNi_{4.73}Sn_{0.27}$ alloys subjected to 30 hydrogen absorption–desorption cycles in the presence of different concentrations of carbon monoxide (100 ppm and 10 ppm) and at different temperatures (40 °C and 90 °C). The results obtained consistently show a strong retardation effect, with no significant capacity loss if samples are allowed enough time to complete the reaction. This observation differs from those of other authors, which indicate a poisoning behavior for this system with a fast loss of capacity. This discrepancy was discussed in terms of experimental conditions and kinetic observations.

For the Sn-containing alloys, a stationary state is met after about 10 cycles, with no further degradation occurring past this point. The retarding factor at 40 °C and 100 ppm in this condition, with respect to the kinetics in pure hydrogen, is of about 600. The kinetics observed at 90 °C during this stationary state is about 10 times faster than that obtained at 40 °C. The kinetics observed at 40 °C in the presence of a CO concentration of 10 ppm is about 100 times faster than that observed under 100 ppm of CO. For $LaNi_5$ the stationary condition is not met after 30 cycles, and the absorption curves resemble those obtained for $LaNi_{4.73}Sn_{0.27}$ during the early, non-stationary stages of the cycling process.

The results suggest that a fraction of the adsorbed CO is released during the desorption process. This effect is stronger at high temperature and could explain most of the different observed kinetic behaviors. The exception is a retardation-recovery effect observed for $LaNi_{4.73}Sn_{0.27}$ cycled at 90 °C and 10 ppm CO which cannot be explained by this effect alone and could be related to the formation of CH_4 on the samples' surface.

The final capacity and kinetic behavior of these materials reach a steady-state after some cycles, allowing them to be considered for possible applications. Material selection and process design should be performed taking into account the different sorption behavior under working conditions. Higher temperatures lead to faster reaction kinetics. The release of traces of adsorbed contaminants (CO, CH_4) should also be considered.

Acknowledgments

The authors acknowledge the help of S. Rivas, F. Roldán, E. Aburto and M. Isla for their help in the preparation of samples

and equipment construction. C. Osuna performed the alloys chemical analysis. This work has been supported by ANPCyT (PAE 36985 and PICT 2012-1796) and by ANPCyT-CNEA through fellowships from PFDT-PRH 200.

REFERENCES

[1] Dunikov D, Borzenko V, Malyshenko S. Influence of impurities on hydrogen absorption in a metal hydride reactor. Int J Hydrogen Energy 2012;37:13843–8.
[2] Sandrock GD, Goodell PD. Cyclic life of metal hydrides with impure hydrogen: overview and engineering considerations. J Less-Common Met 1984;104:159–73.
[3] US DOE. Fuel cell handbook. Morgantown, West Virginia. 5th ed. 2000. p. I–1, I–2, III-11.
[4] Majlan EH, Daud WRW, Iyuke SE, Mohamad AB, Kadhum AAH, Mohammad AW, et al. Hydrogen purification using compact pressure swing adsorption system for fuel cell. Int J Hydrogen Energy 2009;34:2771–7.
[5] Sandrock GD, Goodell PD. Surface poisoning of $LaNi_5$, FeTi and (Fe,Mn)Ti by O_2, CO and H_2O. J Less-Common Met 1980;73:161–8.
[6] Sakaguchi H, Tsujimoto T, Adachi G. The confinement of hydrogen in $LaNi_5$ by poisoning of the hydride surface. J Alloys Compd 1995;223:122–6.
[7] Eisenberg FG, Goodell PD. Cyclic response of reversible hydriding alloys in hydrogen containing carbon monoxide. J Less-Common Met 1983;89:55–62.
[8] Gamo T, Moriwaki Y, Yanagihara N, Iwaki T. Life properties of Ti-Mn alloy hydrides and their hydrogen purification effect. J Less-Common Met 1983;89:495–504.
[9] Han S, Zhang X, Shi S, Tanaka H, Kuriyama N, Taoka N, et al. Experimental and theoretical investigation of the cycle durability against CO and degradation mechanism of the $LaNi_5$ hydrogen storage alloy. J Alloys Compd 2007;446–447:208–11.
[10] Shaltiel D, von Waldkirch Th, Stucki F, Schlapbach L. Ferromagnetic resonance in hydrogenated-dehydrogenated $LaNi_5$, FeTi and Mg_2Ni and its relation to magnetic and surface investigations. J Phys F Metal Phys 1981;11:471–85.
[11] Surnev L, Xu Z, Yates JT. IRAS study of the adsorption of CO on Ni(111): interrelation between various bonding modes of chemisorbed CO. Surf Sci 1988;201:1–13.
[12] Uchida H. Surface processes of H_2 on rare earth based hydrogen storage alloys with various surface modifications. Int J Hydrogen Energy 1999;24:861–9.
[13] Szuber J, Gzempik G, Larciprete R, Koziej D, Adamowicz B. XPS study of the L-CVD deposited SnO_2 thin films exposed to oxygen and hydrogen. Thin Solid Films 2001;391:198–203.
[14] Sato M, Uchida H, Stange M, Yartys VA, Kato S, Ishibashi Y, et al. H_2 reactivity on the surface of $LaNi_{4.7}Sn_{0.3}$. J Alloys Compd 2005;402:219–23.
[15] Au M, Chen C, Ye Z, Fang T, Wu J, Wang O. The recovery, purification, storage and transport of hydrogen separated from industrial purge gas by means of mobile hydride containers. Int J Hydrogen Energy 1996;21:33–7.
[16] Miura S, Fujisawa A, Ishida M. A hydrogen purification and storage system using metal hydride. Int J Hydrogen Energy 2012;37:2794–9.
[17] Kandavel M, Ramaprabhu S. Hydrogen solubility and diffusion studies of Zr-based AB_2 alloys and sol-gel encapsulated AB_2 alloy particles. Intermetallics 2007;15:968–75.
[18] Nishimiya N, Suzuki M, Ishigaki K, Kashimura K. Water resistant hydrogen storage materials comprising encapsulated metal hydrides. Int J Hydrogen Energy 2007;32:661–5.
[19] Fernández GE, Rodríguez D, Meyer G. Hydrogen absorption kinetics of $MmNi_{4.7}Al_{0.3}$. Int J Hydrogen Energy 1998;23(12):1193–6.
[20] Ren J, Williams M, Lototskyy M, Davids W, Ulleberg Ø. Improved tolerance of Pd/Cu-treated metal hydride alloys towards air impurities. Int J Hydrogen Energy 2010;35:8626–30.
[21] Williams M, Lototsky MV, Davids MW, Linkov V, Yartys VA, Solberg JK. Chemical surface modification for the improvement of the hydrogenation kinetics and poisoning resistance of TiFe. J Alloys Compd 2011;509:S770–4.
[22] Wang X-L, Iwata K, Suda S. Hydrogen purification using fluorinated $LaNi_{4.7}Al_{0.3}$ alloy. J Alloys Compd 1995;231:860–4.
[23] Uchida H, Inoue T, Tabata T, Seki S, Uchida HH, Aono F, et al. Effect of HF pretreatment on H reactivity with $LaNi_5$ and $LaNi_{4.7}Al_{0.3}$. J Alloys Compd 1997;253–254:547–9.
[24] Rodriguez DS, Meyer G. Improvement of the activation stage of $MmNi_{4.7}Al_{0.3}$ hydride-forming alloys by surface fluorination. J Alloys Compd 1999;293-295:374–8.
[25] Williams M, Nechaev AN, Lototsky MV, Yartys VA, Solberg JK, Denys RV, et al. Influence of aminosilane surface functionalization of rare earth hydride-forming alloys on palladium treatment by electroless deposition and hydrogen sorption kinetics of composite materials. Mater Chem Phys 2009;115:136–41.
[26] Lototsky MV, Williams M, Yartys VA, Klochko YV, Linkov VM. Surface-modified advanced hydrogen storage alloys for hydrogen separation and purification. J Alloys Compd 2011;509:S555–61.
[27] Lototskyy M, Modibane KD, Williams M, Klochko Y, Linkov V, Pollet BG. Application of surface-modified metal hydrides for hydrogen separation from gas mixtures containing carbon dioxide and monoxide. J Alloys Compd 2013;580:S382–5.
[28] Prigent J, Latroche M, Leoni E, Rohr V. Hydrogen trapping properties of Zr-based intermetallic compounds in the presence of CO contaminant gas. J Alloys Compd 2011;509:S801–3.
[29] Shihai G, Guoqing W, Dongliang Z, Yanghuan Z, Xinlin W. Study on hydrogen in mixed gas separated by rare earth hydrogen storage alloys. Rare Metal Mat Eng 2011;40:189–94.
[30] Borzone EM, Baruj A, Blanco MV, Meyer GO. Dynamic measurements of hydrogen reaction with $LaNi_{5-x}Sn_x$ alloys. Int J Hydrogen Energy 2013;38:7335–43.
[31] Blanco MV, Borzone EM, Baruj A, Meyer GO. Hydrogen sorption kinetics of La-Ni-Sn storage alloys. Int J Hydrogen Energy 2014;39:5858–67.
[32] Borzone EM, Blanco MV, Baruj A, Meyer GO. Stability of $LaNi_{5-x}Sn_x$ cycled in hydrogen. Int J Hydrogen Energy; 2014. http://dx.doi.org/10.1016/j.ijhydene.2013.12.031.
[33] Schweppe F, Martin M, Fromm E. Hydrogen absorption of $LaNi_5$ powders precovered with O_2, CO, H_2S, CO_2 or N_2. J Alloys Compd 1997;253–254:511–4.
[34] Han JI, Lee J-Y. The effect of CO impurity on the hydrogenation properties of $LaNi_5$, $LaNi_{4.7}Al_{0.3}$ and $MnNi_{4.5}Al_{0.5}$ during hydriding-dehydriding cycling. J Less-Common Met 1989;152:319–27.

[35] Han JI, Lee J-I. Simulation of the degradation behavior of the hydrogen absorption kinetics of $LaNi_5$ under the cyclic operations in H_2-CO and H_2-O_2. J Less-Common Met 1990;157:187–99.
[36] Smith G, Goudy AJ. Thermodynamics, kinetics and modeling studies of the $LaNi_{5-x}Co_x$ hydride system. J Alloys Compd 2001;316:93–8.
[37] An XH, Pan YB, Luo Q, Zhang X, Zhang JY, Li Q. Application of a new kinetic model for the hydriding kinetics of $LaNi_{5-x}Al_x$ ($0 \leq x \leq 1.0$) alloys. J Alloys Compd 2010;506:63–9.
[38] Schweppe F, Martin M, Fromm E. Model on hydride formation describing surface control, diffusion control and transition regions. J Alloys Compd 1997;261:254–8.